

Trapping and manipulation of isolated atoms using nanoscale plasmonic structures

D.E. Chang,¹ J.D. Thompson,² H. Park,^{2,3} V. Vuletić,⁴ A.S. Zibrov,² P. Zoller,⁵ and M.D. Lukin²

¹*Center for the Physics of Information and Institute for Quantum Information,
California Institute of Technology, Pasadena, CA 91125*

²*Department of Physics, Harvard University, Cambridge, MA 02138*

³*Department of Chemistry and Chemical Biology, Harvard University, Cambridge, MA 02138*

⁴*Department of Physics, MIT-Harvard Center for Ultracold Atoms, and Research Laboratory of Electronics,
Massachusetts Institute of Technology, Cambridge, Massachusetts 02139*

⁵*Institute for Quantum Optics and Quantum Information of the Austrian Academy of Sciences, A-6020 Innsbruck, Austria
(Dated: May 22, 2009)*

We propose and analyze a scheme to interface individual neutral atoms with nanoscale solid-state systems. The interface is enabled by optically trapping the atom via the strong near-field generated by a sharp metallic nanotip. We show that under realistic conditions, a neutral atom can be trapped with position uncertainties of just a few nanometers, and within tens of nanometers of other surfaces. Simultaneously, the guided surface plasmon modes of the nanotip allow the atom to be optically manipulated, or for fluorescence photons to be collected, with very high efficiency. Finally, we analyze the surface forces and heating and decoherence rates acting on the trapped atom.

Much interest has recently been directed towards hybrid systems that integrate isolated atomic systems with solid-state devices [1, 2, 3, 4]. These efforts are aimed at combining the best of both worlds, namely the excellent coherence and control associated with isolated atoms, ions and molecules, with the miniaturization and integrability associated with solid-state devices. A key ingredient for such integrated devices is the ability to trap, coherently manipulate, and measure individual cold atoms at distances below ~ 100 nm from solid-state surfaces.

In this Letter, we describe a technique that allows a single atom to be optically trapped within a nanoscale region above the surface of a sharp, conducting nanotip. Under illumination with a single blue-detuned laser beam, the nanotip behaves as a “lightning rod” that generates very large field gradients and an intensity minimum that can be used to tightly trap an atom. Simultaneously, the nanotip supports a set of tightly guided surface plasmon modes to which the trapped atom can very efficiently couple. Under realistic conditions, the strong coupling regime can be reached, where the emission rate into the guided surface plasmons of the nanotip far exceeds that into all other channels. It has been shown that this regime enables efficient fluorescence collection and optical manipulation at a single-photon level [5, 6, 7]. Finally, we analyze in detail surface effects and photon scattering and their effects on trap lifetimes and atomic coherence times.

The trapping technique described in this Letter might enable the realization of several unique applications. For example, the nanotrap can be used for deterministic positioning of single atoms near micro-photonic and nano-photonic structures, such as micro-toroidal resonators [8, 9] and photonic crystal cavities [10] (see Fig. 1a). Alternatively, the trap can be used for realization of hybrid quantum systems consisting of single atoms or molecules in the immediate proximity of

charged or magnetized solid-state quantum systems, to enable direct strong coupling [11]. Finally, a trapped atom might be used as a novel scanning probe for sensing magnetic or electric fields with nanoscale resolution. We note that forces associated with metallic systems are being explored, in the context of optical tweezers for dielectric objects on surfaces [12] and electro-optical atomic trapping using nanotubes [13]. In contrast to the latter work, our scheme offers an all-optical trapping method, an open geometry [14], and an efficient mechanism for optical readout and manipulation.

We first derive the optical trapping potential experienced by an atom in the vicinity of the nanotip, whose surface is parameterized by a paraboloid of revolution with rotational axis along z , $z(\rho) = -z_0 + \rho^2/4z_0$. Here z_0 characterizes the curvature of the tip and $\rho = \sqrt{x^2 + y^2}$ is the radial coordinate (see Fig. 1b for an illustration of a tip with $z_0 = 2$ nm). The end of the nanotip is thus located at $z = -z_0$ (the offset from $z = 0$ is conventional in the transformation to paraboloidal coordinates that facilitates analysis). We consider the total field produced by a plane wave incident upon the nanotip from the far field, $\mathbf{E}_{\text{inc}}(\mathbf{r}) = E_0 e^{ik_L x - i\omega_L t} \hat{z}$, which is polarized along the nanotip axis. While an exact analytical solution cannot be obtained for this geometry, the near field around a sub-wavelength nanotip can be approximated using electrostatic equations that do admit analytical solutions [5]. Within this approximation, the total field in the region outside the nanotip is given by

$$\mathbf{E}_{\text{total}} = E_0 \left(1 + \frac{z_0}{r} (\epsilon_L - 1) \right) \hat{z} + \frac{E_0 z_0}{r(r - z)} (1 - \epsilon_L) \boldsymbol{\rho}, \quad (1)$$

while the field inside the nanotip is uniformly $\mathbf{E}_{\text{total}} = E_0 \hat{z}$. Here $\epsilon_L \equiv \epsilon(\omega_L)$ is the dimensionless electric permittivity of the nanotip at the laser frequency (we assume that the surrounding material is vacuum, $\epsilon = 1$) and $r = \sqrt{\rho^2 + z^2}$. When the nanotip is conducting and

far below its plasma resonance, such that $\epsilon_L \ll -1$, the field $\mathbf{E}_{\text{total}} = \epsilon_L E_0 \hat{z}$ at the tip end is greatly enhanced and out of phase relative to the incident field. This is essentially the “lightning rod” effect of a good conductor [15]. Far away from the tip the field must relax back to E_0 and the total field passes zero at $z_{\text{trap}} = z_0(\epsilon_L - 1)$. A small residual field remains if ϵ_L has a small imaginary component ($\epsilon_L \approx -30 + 0.4i$ in silver at wavelength $\lambda_L = 780$ nm [16]). The induced field also varies rapidly near the tip, on a length scale characterized by $|z_{\text{trap}}|$ that can be much smaller than the optical wavelength.

For a simple two-level atom, the field minimum provides a trapping potential when the laser is blue-detuned from the transition frequency ω_a ($\delta \equiv \omega_L - \omega_a > 0$), such that the atomic polarizability is negative. Expanding the fields linearly around the trap center, the potential corresponds to that of a harmonic oscillator, whose trapping frequency $\omega_{T,z}$ along z is given by

$$\hbar\omega_{T,z} = 2\sqrt{\frac{\hbar\Omega_0^2}{\delta}}E'_R, \quad (2)$$

where $E'_R = E_R(k_a z_{\text{trap}})^{-2}$ is an effective “enhanced” recoil energy relative to the recoil energy $E_R = \hbar^2 k_a^2 / 2m$ in free space, m is the mass of the atom, $k_a = \omega_a / c$, and Ω_0 is the Rabi frequency associated with the incident field amplitude. The ground-state uncertainty of the trap along z is $a_z = \sqrt{\hbar / 2m\omega_{T,z}}$, while the trap frequency in the radial directions is $\omega_{T,\rho} = \omega_{T,z} / 2$. Note that the field gradients created by the nanotip strongly enhance E'_R , such that larger trap frequencies $\omega_{T,z} \propto 1/|z_{\text{trap}}|$ can be obtained for a given input intensity.

An atom trapped in this nanoscale region can be optically manipulated and read out with near unit efficiency via efficient coupling of the atom to guided surface plasmons (SPs) that propagate along the nanotip surface. Following the ideas of Ref. [17], a large coupling strength between a single SP (*i.e.*, a single photon) and single atom results when the atom is placed within the SP evanescent field, due to the sub-diffraction limit confinement of the SPs. This effect yields an enhanced spontaneous emission rate Γ_{pl} into the SPs over the rate Γ' into all other channels, which can be characterized by an “effective Purcell factor” $P = \Gamma_{\text{pl}} / \Gamma'$. To illustrate this effect, the Purcell factor for an atom (emission wavelength at $\lambda_a = 780$ nm) trapped at position $z = z_{\text{trap}}$ near a silver nanotip is plotted in Fig. 2a as a function of z_0 . It can be seen that the strong coupling regime $P > 1$ can be achieved over a realistic range of z_0 . Furthermore, the strong coupling is broadband and associated primarily with the small tip size, and thus no special tuning of the nanotip is required to achieve the strong coupling for some particular atom.

For realistic parameters, the distance $d = |\epsilon_L|z_0$ between the trap center and tip surface is on the order of tens of nanometers (see Fig. 2a), and thus surface ef-

fects can play an important role in the trap characteristics. Here we identify and analyze several prominent surface effects – an attractive van der Waals force from the nanotip and “patch potentials” caused by adatoms that modify the total potential experienced by the atom, and magnetic field fluctuations caused by “polarization noise” in the nanotip that induce both motional heating and hyperfine state flips in a multilevel atom. The van der Waals force can be calculated classically based on the interaction between an oscillating dipole \mathbf{d} at some point \mathbf{r} and its own reflected field [18]. This calculation is valid when $k_a d \lesssim 1$ (such that retardation is not important), which is true for our cases of interest. Taking the known result for the field reflected from a nanotip [5], the van der Waals potential as $z \rightarrow -z_0$ is given for a two-level atom by $U_{\text{vdW}}(z) \approx -\frac{3\hbar\Gamma_0}{32k_a^3 d^3}$, where Γ_0 is the free-space spontaneous emission rate. U_{vdW} is attractive and diverges with the usual d^{-3} scaling as the distance to the surface d approaches zero. For sufficiently weak optical potentials, the total potential $U_{\text{opt}} + U_{\text{vdW}}$ may cease to support a trapping minimum away from the surface. The condition for a trap to exist is approximately

$$\frac{\Omega_0^2}{\delta} \gtrsim \frac{9\Gamma_0}{32(k_a |z_{\text{trap}}|)^3}, \quad (3)$$

i.e., the strength of the laser potential should roughly exceed that of the van der Waals force at the trap position. Even if the condition above is satisfied, some probability remains for the atom to tunnel from the local trapping minimum to the surface. However, the tunneling rate is exponentially suppressed with barrier height and can be ignored once Eq. (3) is even moderately satisfied.

A second correction to the total potential occurs if additional adatoms (in addition to the trapped atom) become adsorbed to the nanotip surface [19]. Each adatom forms a static dipole moment p_0 due to its electronic wave function being pulled into or away from the surface, thus producing a small static electric field. The total static field E_p in turn creates an additional “patch” potential for the trapped atom, $U_p = -(1/2)\alpha_s E_p^2$, where α_s is the atomic static polarizability. Assuming that a uniform monolayer of adatoms substitute themselves over some portion of the nanotip surface, it is straightforward to show that the maximum force (*i.e.*, in a worst-case scenario) at a distance d away from the nanotip is given by $F_p(d) \lesssim 0.1 \frac{p_0^2 z_0^2 \alpha}{\epsilon_0^2 d^5 a^4}$, where a is the lattice spacing of the nanotip material. For typical dipole moments of $p_0 \sim 1$ Debye, this force shifts the trap center only by an amount comparable to the size of the ground-state wavepacket near the minimum intensities needed to overcome the van der Waals potential (Eq. (3)). Thus from this point forward we will ignore the possibility of patch potentials in our calculations.

Eq. (3) predicts that the minimum amount of incident laser intensity needed to support a trap rises rapidly

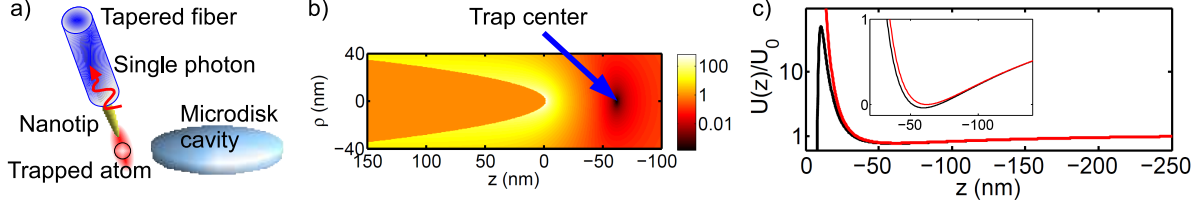


FIG. 1: a) Schematic of a single atom tightly trapped near a conducting nanotip. The atom is strongly coupled to single surface plasmons guided by the nanotip, which can be efficiently converted to a single photon in a coupled optical fiber, allowing for efficient manipulation and read-out. The atom can be brought within tens of nanometers of other surfaces, which allows it to be interfaced, *e.g.*, with an optical microdisk cavity as shown here. b) Illustration of a nanotip with $z_0 = 2$ nm and normalized total field intensity $|E_{\text{total}}/E_0|^2$. c) Typical optical potential (red) and total potential (including van der Waals potential, black) for a Rb atom trapped near a $z_0 = 2$ nm nanotip. The potentials are normalized by $U_0 = \hbar\Omega_0^2/\delta$, the optical potential at infinity. The inset shows the potentials around the trap center in greater detail.

with decreasing nanotip size. On the other hand, for sufficiently large intensities the laser power absorbed by the nanotip, as determined by the imaginary part of ϵ_L , will cause it to melt. Assuming that the nanotip has a good thermal contact conductance (*e.g.*, comparable to achievable values for wires in atom chips [20]) with some substrate, we estimate that incident laser intensities exceeding $10 \text{ mW}/\mu\text{m}^2$ can be used for silver nanotips at $\lambda_L = 780 \text{ nm}$ [21]. These two considerations set a lower bound for the tip size z_0 of around hundreds of picometers. An upper bound for z_0 is set by the validity of our electrostatic calculations. Specifically, in a subwavelength region around the end of the tip, the tip profile must appear “sharp” (as defined by having a large aspect ratio of $z/2\rho$), and the trap distance should satisfy $k_a d \lesssim 1$, which places an upper limit to z_0 of several nanometers.

We now discuss the limitations on atomic coherence times and trap lifetimes. First, the proximity of the trap to the surface makes the atom susceptible to magnetic field noise \mathbf{B}_N induced by material losses in the nanotip. This field noise couples to the electron spin via the Hamiltonian $V = -\mu_B g_S \mathbf{S} \cdot \mathbf{B}_N(\mathbf{r}, t)$, resulting in incoherent transitions between ground-state hyperfine levels and jumps between trap motional states. Here μ_B is the Bohr magneton and g_S is the electron spin g-factor. An analytical solution for \mathbf{B}_N cannot be found for the nanotip. However, to estimate its effect, we can consider an atom sitting a distance d above a semi-infinite substrate of the same permittivity as the nanotip. The hyperfine transition rate $\Gamma_{\Delta F, \text{mag}}$ and motional jump rate $\Gamma_{\text{jump, mag}}$ due to magnetic noise in this case are $\Gamma_{\Delta F, \text{mag}} \propto \frac{(\mu_0 \mu_B g_S)^2}{\hbar^2 \rho d} k_B T$, $\Gamma_{\text{jump, mag}} \propto \Gamma_{\Delta F, m} (a_z/d)^2$ [22] where ρ is the resistivity of the nanotip. We note that the semi-infinite substrate overestimates the amount of polarizable material and that for realistic tips the noise should be reduced by a factor

of order $\sim (z_0/z_{\text{trap}})^2$. The hyperfine transitions result only in a loss of internal atomic coherence, since all hyperfine states can be trapped in the optical fields. In the following we assume that the nanotip roughly sits at room temperature, $T \sim 300 \text{ K}$.

Analogous processes occur due to inelastic scattering of photons from the trapping field. Because of the tight trap confinement, the change in motional state primarily consists of events where a single phonon is added or subtracted, in analogy with heating of ions in the Lamb-Dicke limit [23]. The transition rates can generally be obtained by second-order perturbation theory [24, 25]. For a two-level system, we find a jump rate

$$\Gamma_{\text{jump, opt}} \approx \Gamma_{\text{total}}^{(z)} \frac{E'_R}{\hbar \omega_{T,z}} \frac{\Omega_0^2}{\delta^2}, \quad (4)$$

where $\Gamma_{\text{total}}^{(z)}$ denotes the total spontaneous emission rate for a dipole oriented along the nanotip axis. Note that the enhanced recoil energy E'_R yields a larger heating rate as compared to free space. Photon scattering also results in hyperfine transitions, which we calculate using analogous techniques [25]. An additional source of heating is laser shot noise, which causes fluctuations in the trap frequency ω_T . For a laser beam focused to $\sim \lambda^2$, however, this heating is smaller than $\Gamma_{\text{jump, opt}}$ by a factor $\sim (a_z/d)^2$.

As a numerical example, we now consider the trapping of individual ^{87}Rb atoms ($\lambda_a \sim 780 \text{ nm}$ for the D2 line, $\Gamma_0 \sim 38 \text{ MHz}$, saturation intensity $I_{\text{sat}} \sim 1.7 \text{ mW}/\text{cm}^2$) near a silver nanotip. For the nanotip heating rates calculated previously, traps with laser intensities of up to $I \sim 10^9 I_{\text{sat}}$ can be realized. In these examples, both the complex value of ϵ_L and the multilevel atomic structure of Rb have been fully accounted for. For the latter consideration, the optical interactions include the atomic fine structure, and are averaged assuming that all magnetic states m_F are trapped with equal populations. In Fig. 2b

we plot the trap lifetime for various values of $\omega_{T,z}$ and z_0 . The incident field intensity is shown along the horizontal axis, while the detunings are varied to yield the desired values of $\omega_{T,z}$. The black dashed (solid) curve corresponds to a nanotip of $z_0 = 3$ nm and trap frequency of $\omega_{T,z} = 10$ (100) MHz, while the red curve corresponds to $z_0 = 1$ nm and $\omega_{T,z} = 100$ MHz. Note that $\omega_{T,z} = 100$ MHz corresponds to a ground-state localization of $a_z \sim 2$ nm. The van der Waals force has been accounted for in calculating the total potential, and the trap lifetime is the time it takes for the energy of the atom to exceed the depth of the total potential. For the $\omega_{T,z} = 10$ MHz curve, trap lifetimes exceeding ~ 1 s can be readily achieved. At the same time, spin flip times (dominated by magnetic field noise at large detunings $\delta \sim 10^6 \Gamma_0$) are conservatively calculated to be around 10 ms using the results obtained for a semi-infinite substrate; however, by estimating a correction based on the small solid angle actually spanned by the nanotip, we believe that times on the order of a second are possible. In the regime where the van der Waals potential does not perturb the trap significantly, the trapped atom sits 90 (30) nm from the tip surface for a tip curvature of $z_0 = 3$ (1) nm, giving a corresponding Purcell factor of $P \sim 0.2$ (6) when averaged over dipole orientations.

Loading the nanotip trap can be accomplished starting with an atom initially trapped within a few-micron vicinity of the nanotip in a separate, far-field red-detuned optical dipole trap. Suppose in particular that the far-field trapping beam is polarized perpendicular to the nanotip axis (say along \hat{x}). A similar analysis as above shows that the total field for a plane wave along the nanotip axis is given by $\mathbf{E}_{\text{total}} = E_0 \left(1 + \frac{1-\epsilon_L}{1+\epsilon_L} \frac{z_0}{|z|}\right) \hat{x}$. Thus, for this polarization, the incident field is only modified at very close distances to the tip of order $z_{\perp} \sim z_0(\epsilon_L - 1)/(\epsilon_L + 1) \ll |z_{\text{trap}}|$, *i.e.*, the nanotip has minimal effect on the far-field trap. The atom can then be loaded into our system by adiabatically switching on (off) the nanotip (far-field) trap. The different responses of the two polarizations ensures that the trapping potentials of the red- and blue-detuned beams do not simply cancel each other out in the loading process.

In summary, we have described a technique that allows for the nanoscale trapping and efficient optical manipulation of single atoms on a chip. Such a trap is expected to display long trap lifetimes and atomic coherence times, and its open geometry and large depth allow the trapped atom to be brought into close proximity (~ 50 nm) of other surfaces as well. The combination of these features potentially opens up many exciting opportunities. For example, the nanotip could be used to trap atoms within the evanescent field modes of optical resonators such as whispering-gallery mode resonators [8, 9] and photonic crystal cavities [10]. The nanotip may also be used as a scanning tip for weak-field sensing near surfaces. In

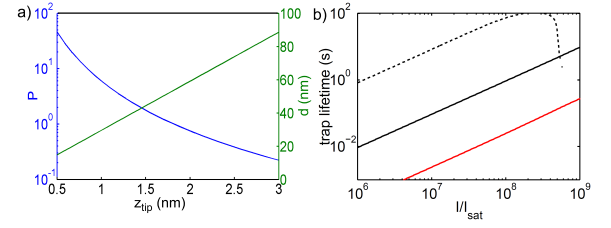


FIG. 2: a) Purcell factor P (averaged over dipole orientations, blue curve) and trap distance to surface d (green curve) for a ^{87}Rb atom trapped near a silver nanotip, as a function of z_0 , in absence of van der Waals forces. b) Trap lifetime for various values of trapping frequency $\omega_{T,z}$ and tip curvature z_0 . The incident trap laser intensity is plotted along the horizontal axis, while the detuning is varied to maintain a given value of $\omega_{T,z}$. The black dashed (solid) curve corresponds to $z_0 = 3$ nm and trap frequency of $\omega_{T,z} = 10$ (100) MHz, while the red curve corresponds to $z_0 = 1$ nm and $\omega_{T,z} = 100$ MHz.

magnetometry, for example, the field sensitivity will be determined by the atomic spin coherence time T_2 . Estimating coherence times of $T_2 \sim 1$ s yield ultimate magnetic field sensitivities of $\delta B \sim \hbar / g_S \mu_B \sqrt{T_2} \sim 20$ pT/ $\sqrt{\text{Hz}}$, which compare favorably with spins localized in solid state [26]. Furthermore, the tight trapping is expected to give rise to novel atomic interactions. If two atoms are trapped simultaneously, the ground-state uncertainties can be made comparable to the length scale over which they experience a van der Waals interaction [27]. In this regime, optical forces could directly “push” on a molecule and alter its properties and dynamics. Also, arrays of nanotips could form optical lattices with very small lattice constants, enabling the exploration of novel many-body physics [28]. Finally, these ideas could also be extended to other systems of interest, such as polar molecules [2] or ions [23].

This work was supported by the NSF, Harvard-MIT CUA, DARPA, and Packard Foundation. DEC acknowledges support from the Gordon and Betty Moore Foundation through Caltech’s Center for the Physics of Information, and the National Science Foundation under Grant No. PHY-0803371.

-
- [1] C. Monroe and M. D. Lukin, Phys. World pp. 32–39 (2008).
 - [2] A. André, D. Demille, J. M. Doyle, M. D. Lukin, S. E. Maxwell, P. Rabl, R. J. Schoelkopf, and P. Zoller, Nature Phys. **2**, 636 (2006).
 - [3] R. Folman, P. Kruger, J. Schmiedmayer, J. Denschlag, and C. Henkel, Adv. At. Mol. Opt. Phys **48**, 263 (2002).
 - [4] P. Treutlein, T. Steinmetz, Y. Colombe, B. Lev, P. Hommelhoff, J. Reichel, M. Greiner, O. Mandel, A. Widera, T. Rom, et al., Fortschr. Phys. **54**, 702 (2006).

- [5] D. E. Chang, A. S. Sørensen, P. R. Hemmer, and M. D. Lukin, Phys. Rev. B **76**, 035420 (2007).
- [6] D. E. Chang, A. S. Sørensen, E. A. Demler, and M. D. Lukin, Nature Phys. **3**, 807 (2007).
- [7] A. V. Akimov, A. Mukherjee, C. L. Yu, D. E. Chang, A. S. Zibrov, P. R. Hemmer, H. Park, and M. D. Lukin, Nature **450**, 402 (2007).
- [8] Vahala, K. J., Nature **424**, 839 (2003).
- [9] T. Aoki, B. Dayan, E. Wilcut, W. P. Bowen, A. S. Parkins, T. J. Kippenberg, K. J. Vahala, and H. J. Kimble, Nature **443**, 671 (2006).
- [10] J. Vučković and Y. Yamamoto, Appl. Phys. Lett. **82**, 2374 (2003).
- [11] P. Treutlein, D. Hunger, S. Camerer, T. W. Hänsch, and J. Reichel, Phys. Rev. Lett. **99**, 140403 (2007).
- [12] M. Righini, A. S. Zelenina, C. Girard, and R. Quidant, Nature Phys. **3**, 477 (2007).
- [13] B. Murphy and L. V. Hau, Phys. Rev. Lett. **102**, 033003 (2009).
- [14] R. Maiwald, D. Leibfried, J. Britton, J. C. Bergquist, G. Leuchs, and D. J. Wineland, ArXiv e-prints (2008), 0810.2647.
- [15] J. D. Jackson, *Classical Electrodynamics, 3rd ed.* (John Wiley & Sons, New York, 1999).
- [16] P. B. Johnson and R. W. Christy, Phys. Rev. B **6**, 4370 (1972).
- [17] D. E. Chang, A. S. Sørensen, P. R. Hemmer, and M. D. Lukin, Phys. Rev. Lett. **97**, 053002 (2006).
- [18] R. R. Chance, A. Prock, and R. Silbey, Phys. Rev. A **12**, 1448 (1975).
- [19] J. M. McGuirk, D. M. Harber, J. M. Obrecht, and E. A. Cornell, Phys. Rev. A **69**, 062905 (2004).
- [20] S. Groth, P. Krüger, S. Wildermuth, R. Folman, T. Fernholz, J. Schmiedmayer, D. Mahalu, and I. Bar-Joseph, Appl. Phys. Lett. **85**, 2980 (2004).
- [21] This calculation of the maximum intensity is consistent with preliminary experiments involving silver nanowires, where green laser light with intensities exceeding $10 \text{ mW}/\mu\text{m}^2$ have been found to not melt the nanowires.
- [22] C. Henkel, S. Pötting, and M. Wilkens, Appl. Phys. B **69**, 379 (1999).
- [23] D. Leibfried, R. Blatt, C. Monroe, and D. Wineland, Rev. Mod. Phys. **75**, 281 (2003).
- [24] D. J. Wineland and W. M. Itano, Phys. Rev. A **20**, 1521 (1979).
- [25] R. A. Cline, J. D. Miller, M. R. Matthews, and D. J. Heinzen, Opt. Lett. **19**, 207 (1994).
- [26] J. M. Taylor, P. Cappellaro, L. Childress, L. Jiang, D. Budker, P. R. Hemmer, A. Yacoby, R. Walsworth, and M. D. Lukin, Nature Phys. **4**, 810 (2008).
- [27] E. L. Bolda, E. Tiesinga, and P. S. Julienne, Phys. Rev. A **66**, 13403 (2002).
- [28] I. Bloch, J. Dalibard, and W. Zwerger, Rev. Mod. Phys. **80**, 885 (2008).